Proceedings of the ASME 2010 Pressure Vessels & Piping Division / K-PVP Conference
PVP2010
July 18-22, 2010, Bellevue, Washington, USA

PVP2010-25735

MONTE CARLO SIMULATION FOR STRUCTURE OF METALLIC CLUSTERS

Y.H. Park and I. Hijazi
Mechanical & Aerospace Engineering Department
New Mexico State University
Las Cruces, NM 88003

ABSTRACT

The structural stability and energetics for small copper and gold clusters Cu_n and Au_n (n=21-56) were investigated using an effective Monte Carlo simulated annealing method, which employs the Aggregate-Volume-Bias Monte Carlo (AVBMC) algorithm. Incorporated in the Monte Carlo method, is an efficient Embedded Atom Method (EAM) potential developed by the authors. In general agreement with previous empirical studies, the lowest-energy copper structures adapt a single icosahedral structural motif, with pentagonal bipyramid geometry as the building block. However, contrary to studies that describe gold as less symmetric, this work demonstrates that gold clusters adapt both an icosahedral and icositetrahedral structural motifs with many clusters having symmetric geometries.

1. INTRODUCTION

The study of metal clusters has attracted much attention in recent years. Metal nanoclusters containing less than 400 atoms show quantum size effects [1] which give them unique properties. Copper (Cu) and gold (Au) nanoclusters are of particular interest since their chemical, thermodynamic, electronic, and optical properties make them interesting candidates as building blocks of nanostructure materials and nanoelectronic digital circuits [2-4]. Delineation of these properties requires a complete and definitive characterization of the cluster's geometrical structure. The investigation of the structural stability of small metal clusters also has great importance in understanding physical phenomena such as crystal growth and catalysis. The complexity of the potential energy surfaces of some metal clusters leads to a large number of local minima, making localization of the true global minima very difficult.

Several empirical approaches have been used to describe large clusters. The Cu and Au clusters with up to 55 atoms were studied based on empirical potentials. Garcia-Rodeja et al. [6] used Voter and Chen EAM potential to study structures and binding energies of the lowest-energy isomers as well as melting behavior of the Cu_n and Au_n (n=2-23) clusters. They presented stable structures of the 13- and 19- atom clusters for both metals which are icosahedron and double-icosahedron, respectively. Other cluster configurations are obtained from 13-atom cluster configurations by removing or adding surface atoms. Erkoc and Shaltaf [7] investigated the structural stability and energetics for copper clusters up to 55 atoms by using a Monte Carlo technique at room temperature. They found that the majority showed five-fold structures, with Cu_{13} and Cu_{19} being icosahedral and double-icosahedral, respectively. Structures and stability of up to 56 atoms of copper and gold clusters were also employed by Darby et al. [8] using the many-body Gupta potential. In their work, most copper clusters have icosahedron-based geometries. Exceptions to the icosahedral motif occur at around Cu_{40}, where the structures adopt oblate, decahedron-like geometries, and at Cu_{38}, which has an fcc-like truncated octahedral structure. Two-shell centered icosahedral structure was found for Cu_{55}. Gold clusters do not adopt a single structural motif, instead they mostly have low-symmetry structures. Most larger structures are nonicosahedral in nature. Unlike Cu_{55}, Au_{55} has a more amorphous structure. A hexagonal prismatic structural motif was found for Au_{21}. As for copper, Cu_{38} adapted a truncated octahedral structure. Wilson and Johnson [9] applied a molecular dynamics simulated annealing which uses an empirical Murrel Mottram many-body potential to probe the structure and stability of small gold clusters consisting of between 2 and 40 atoms. In their work, no single structural motif dominates the predicted global minima over this size range. They found Au_{21} (triple layer hexagonal prism) and Au_{38} (truncated octahedron) structures to be stable with respect to their neighboring nuclearities.

Some inconsistent results of lower-energy structures especially for gold clusters were observed in previous empirical studies. To resolve these disagreements, we perform a comprehensive theoretical study of the lower-energy structures for Cu and Au nanoclusters in the size range from 21 to 56 atoms. In general, the precise form of the interaction potential and an efficient global optimization algorithm are responsible for the search of low-energy structures for metal clusters. The present study is based on Monte Carlo (MC) simulation with the annealing method, using a recently published efficient Embedded Atom Potential developed by the authors [10].

2. THE POTENTIAL ENERGY FUNCTION

In the theoretical framework of an Embedded Atom Method (EAM) the total energy of a system can be written as [11]

$$E_{tot} = \sum_i F_i(\rho_{h,i}) + \frac{1}{2}\sum_{\substack{i,j \\ (i \neq j)}} \phi_{ij}(r_{ij}) \qquad (1)$$

where E is the total internal energy, $\rho_{h,i}$ is the electron density at atom *i* due to all other atoms, f_j is the electron density of atom *j* as a function of distance from its center, r_{ij} is the separation distance between atoms *i* and *j*, $F_i(\rho_{h,i})$ is the energy to embed atom *i* in an electron density $\rho_{h,i}$, and ϕ_{ij} is a two-body central potential between atoms *i* and *j*. For the embedding function we take the following form suggested by Hijazi and Park [10]

$$F(\rho) = F(\rho_e)\left[1 - \eta \ln\left(\frac{\rho}{\rho_e}\right)\right]\left(\frac{\rho}{\rho_e}\right)^{\eta} \quad (2)$$

We also assume that the atomic electron density has the following exponential form:

$$f = f_e e^{-\chi(r-r_e)} \quad (3)$$

where f_e is a scaling constant, and r_e is the equilibrium nearest distance, and χ is a parameter to be decided. The two-body potential is taken as follows:

$$\phi = -\phi_e\left[1 + \delta(r/r_e - 1)\right]e^{-\beta(r/r_e - 1)} \quad (4)$$

This function has three adjustable parameters, ϕ_e, δ, and β. These analytical functions are easy to be implemented in a computer simulation. In principle, they can be used for any crystal structure. For the materials Au and Cu the value of the five adjustable parameters χ, ϕ_e, β, η, and ρ_e used in this work are listed in Table 1.

Table 1: Fitting parameters for Cu and Au.

Metal	χ	φ	δ	β	η	ρ_e
Au	3.4991	0.1296	8.4781	7.6013	0.5640	2.6836
Cu	2.4351	0.1751	8.7919	6.9336	0.5736	3.6728

3. MONTE CARLO SIMULATION METHOD

The precision of the present simulation results depends on the extent to which the space of the system is sampled throughout the simulation. In this Monte Carlo simulation the *NVT* canonical ensemble is used. The simulation procedure utilizes the standard Metropolis Algorithm as well as the Aggregate-Volume-Bias Monte Carlo (AVBMC) algorithm.

3.1 Metropolis translation move

Starting from a given configuration of the system, state *A*, the Metropolis translation move proceeds as follows:

(1) Chose an atom *i* at random to be moved.
(2) Chose a vector on a unit sphere at random and then attempt to displace atom *i* a random distance between $-r_{max}$ and $+r_{max}$ in that direction, leading to a trial configuration of state *B*.
(3) Calculate the potential energy difference, $\Delta E = E_B - E_A$ and accept this move with a probability of

$$acc(A - B) = \min\left[1, \exp(-\Delta E / K_B T)\right] \quad (5)$$

where K_B and *T* are Boltzmann's constant and the absolute temperature in Kelvin, respectively.

3.2 AVMBC trial move

Whereas the unbiased translational trial move is used to explore nearby regions of phase space, the AVBMC algorithm introduces a trial move useful for forming and destroying clusters with atoms that tend to segregate together [12]. Starting from a given configuration *A*, an AVBMC trial move proceeds as follows:

(1) Chose an atom *i* at random to be moved.
(2) From a bounded region, chose randomly a second atom *j* that serves as the target for the move.
(3) With a probability of $P_{bias,}$ atom *i* is allowed to move only into the bounded region of atom *j*, called the B_{in} state, while with a probability of *1*- $P_{bia, s}$ atom *i* is moved into the nonbonded region of atom *j*, called the B_{out} state.
(4) Calculate the potential energy difference, $\Delta E = E_B - E_A$.
(5) Accept this move with the following set of acceptance probabilities:
   (a) If the swap move does not involve atom *i* entering or leaving the bonded region of atom *j*, the standard Metropolis acceptance rule is used.
   (b) If atom *i* enters the bounded region of atom *j*, the following acceptance rule is used:

$$acc(A_{out} - B_{in}) = \min\left[1, \frac{(1 - P_{bias}) \times V_{in} \times \exp(-\Delta E / K_B T)}{P_{bias} \times V_{out}}\right] \quad (6)$$

   where V_{in} is the volume of the bonded in region and $V_{out} = V - V_{in}$ is the remainder of the system's volume.
   (c) If atom *i* enters the nonbounded region of atom *j*, the following acceptance rule is used:

$$acc(A_{in} - B_{out}) = \min\left[1, \frac{P_{bias} \times V_{out} \times \exp(-\Delta E / K_B T)}{(1 - P_{bias}) \times V_{in}}\right] \quad (7)$$

For each cluster size *N*, the initial geometry was generated by placing *N* atoms at random positions. The Cartesian *x*, *y*, and *z* coordinates are chosen randomly within a sphere of radius $0.5 r_e N^{1/3}$, where r_e is the equilibrium nearest-neighbor distance in the bulk solid. This ensures that the cluster volume scales linearly with the cluster size. The randomly generated initial structure was equilibrated for more than 1,000 Monte Carlo cycles at a given temperature. Thereafter, simulations in the canonical ensemble were carried out for more than 10,000 cycles (one Monte Carlo cycle consists of *N* Monte Carlo moves and *N* is the number of atoms in the system). An annealing run is then performed after each cycle by slightly decreasing the temperature. The cluster is thus slowly cooled by periodically decreasing the temperature. This Monte Carlo procedure has proven to be effective in determining, with good certainty, the global minima within this size range..

4. RESULT AND DISCUSSION

The energy and geometry of the most stable pure copper and gold clusters with the number of atoms n=21-56 were researched. Figures 1 and 2 show the geometry of the most stable copper and gold clusters. The present simulation gives the most stable structures for the copper clusters with the number of atoms n = 21-24 as the icosahedron structures while the Cu_{25} structure was found to be disordered. The icosahedron structure was also found for clusters n = 26, 27, 29, 31, 36 and 39, while for n = 28, 30, 32-35 and 37 the structure was found to be disordered.

.

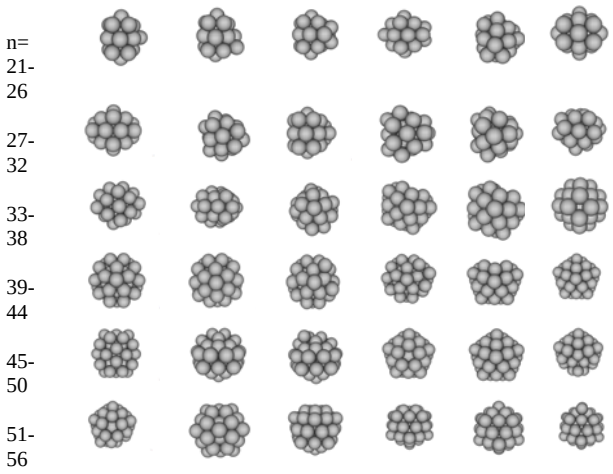

Figure 1. The structure of energetically most stable copper clusters, Cu_n, n = 21-56

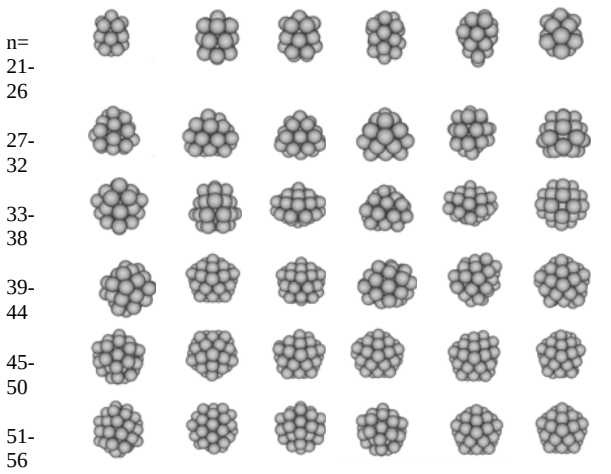

Figure 2. The structure of energetically most stable gold clusters, Au_n, n = 21-56

A highly symmetric fcc-like truncated octahedral (TO) structure forms at Cu_{38}, while for Cu_{40} the structure adopts a flattened, decahedron like geometry. The rest of the larger clusters, n = 41-54, have icosahedron-based geometry, culminating in the complete, two-shell centered icosahedral structure found for n = 55 and 56. It has also been found that the five-fold symmetry is favored in the optimized copper structures.

While copper adopts a single icosahedral structural motif, gold clusters adopt both icosahedron and icositetrahedron structural motifs. The stable structures of the 21-26 atom clusters are obtained from an icositetrahedron configuration by removing or adding surface atoms to the symmetric double icositetrahedron Au_{22}. With the exception of n = 30 and 33 being hexagonal closed pack (hcp) structure and n = 31 being icosahedron, the clusters n = 27-37 have a less defined structure. In the next two clusters, n=38 and 39, the structures are a symmetric truncated fcc structures. While the structure of n = 40 appears to be disordered, the structure of n = 41 is a symmetric hexagonal closed pack. With the exception of n = 48 being an hcp and n = 50 being a symmetric fcc, in the next range, n = 42-53, the pentagonal bipyramid structure becomes dominant while exhibiting a five-fold outer geometry. The next two large gold clusters, n = 54 and 55, have icosahedron-based geometry, culminating in the complete, two-shell centered icosahedral structure found for n = 56.

For copper clusters, the present results are in good agreement with those in reference [7] and [8]. The present results essentially indicate that the majority of the structures displayed have a five-fold surface geometry, in agreement with the two previous studies. The present results for gold clusters *partially* agree with the results of previous empirical methods used by Wilson and Johnston [9] and Darby et al. [8]. We found icosatetrahedron configurations with energies lower than those obtained by Wilson and Johnston and Darby et al. for Au_{22} who found n =21 to be a hexagonal prismic motif in nature, which is in reasonable agreement with the present result. In a previous study of gold clusters, bound by the Murrel-Mottram many-body potentials [9], the authors also found a hexagonal prismic structure for n = 21. For gold clusters, n = 38 and 39, our predicted results of fcc-like truncated octahedral motif is in good agreement with those of Wilson and Johnston [9] and Darby et al. [8].

For n = 55 and 56 our two-shell icosahedral configurations are not in agreement with those of Darby et al. [8]. For n = 55, they predicted an amorphous structure and for n = 56 an fcc-based structure. However, a previous study by Cox et al., [13] predicted a two-shell icosahedral geometry for n = 55.

5. RELATIVE STRUCTURE STABILITY

The relative stabilities of the clusters described earlier can be studied by analyzing their energies. We have considered the evolution of the average interaction energy E_c, the difference in energy in adding an atom to the preceding cluster, that is, the first difference energy $\Delta E^{(1)}$ and the second-order derivative, or the second difference energy $\Delta E^{(2)}$. These energies are defined in terms of the total interaction energy of the cluster with the number of atoms N as, respectively.

$$E_c = \frac{E_{total}}{N} \tag{8}$$

$$\Delta E^{(1)} = E_N - E_{N-1} \tag{9}$$

$$\Delta E^{(2)} = E_{N+1} - 2E_N + E_{N-1} \tag{10}$$

From the above equations, in the limit of very large clusters both E_c and $\Delta E^{(1)}$ will approach the cohesive energy of the corresponding bulk solid as shown in Figure 4 for Cu and Au clusters.

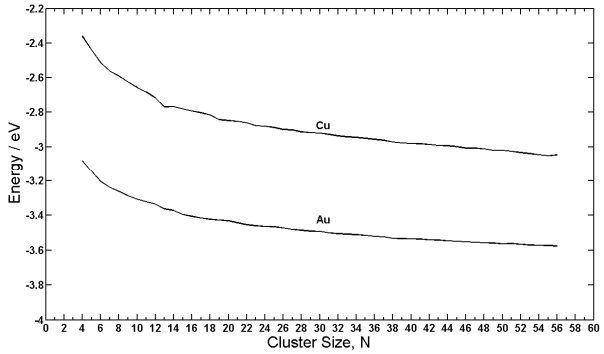

Figure 4. Cohesive energy for Cu and Au clusters.

Figure 5 shows plots of the first and second energy difference calculated for copper. There are significant peaks at n = 6, 13, 19, 23, 26, 28, 38, 43, 46, 49 and 55 which imply greater stability at these nuclearities.

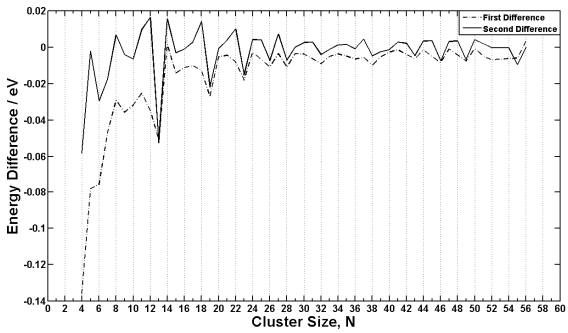

Figure 5. First and second energy difference for Cu clusters.

Figure 6 shows plots for the first and second energy difference for gold. By contrast, while there are still large peaks at n = 13 and 38, for gold clusters, there are significant peaks at n = 6, 15, 22, 27, 31, 38, 50 and 53. Comparing our results with other studies, Darby et al. [18] found significant peaks for copper at n = 7, 13, 19, 23 and 55. For gold they found significant peaks at n = 7, 13, 30 and 38. Erkoc and Shaltaf [7] found in their investigation for copper the lowest-energy magic clusters to be n = 13, 20, 24, 29, 34 and 45. Wilson and Johnston [9] predicted in their study of gold that the most stable structures were n = 6, 8, 13, 17, 26, and 38.

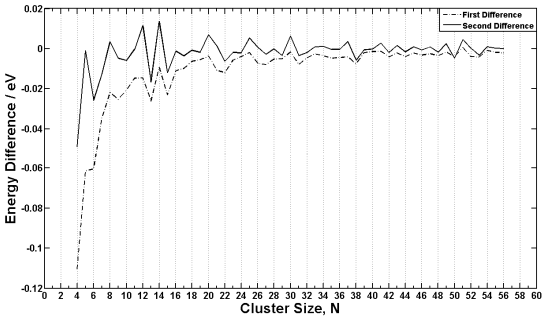

Figure 6. First and second energy difference for Au clusters. gold the most stable structures were predicted to be n = 22, 27, 31, 38, 50 and 53

6. CONCLUSION

The lowest-energy geometrical structures for pure Cu_n and Au_n (n = 21-56) metals were investigated using the AVBMC algorithm. An embedded atom potential function proposed by the authors has been used in the simulation. The lowest-energy structures found are generally based on octahedral, decahedra, icosahedra and hexagonal prisms. For copper n = (21-24, 26, 27, 29, 31, 36, 39, 41-56) the structures were found to be icosahedron and for n = (25, 28, 30, 32-35, 37, 40) the structures were disordered. As for n = 38 an fcc-like truncated octahedral structure was obtained. For gold clusters n = 21-26 the structure was found to be icositetrahedron with Au_{22} being a double icositetrahedron. For n = 41 and 48 a hexagonal closed pack structure was obtained, while for n = 38, 39 and 50 an fcc-like truncated octahedron structure was predicted. For the largest clusters, n = 54-56, the icosahedron was found to be the lowest-energy structure. The most stable copper structures were found to be n = 23, 26, 28, 38, 43, 46, 49 and 55. As for gold the most stable structures were predicted to be n = 22, 27, 31, 38, 50 and 53.

REFERENCE

1. T.G. Schaaff, M.N. Shafigullin, J.T. Khoury, I. Vezmar, RL.L. Whetten, W.G. Gullen, P.N. Fisrt, C. Gutierrez-Wing, J. Ascensio, and M. Jose-Yacaman, J. Phys. Chem. B **101**, 7885 (1997).
2. R.P. Andres, T. Bein, M. Dorogi, S. Feng, J.I. Henderson, C.P. Kubiak, W. Mahoney, R.G. Osifchin, and R. Reifenberger, Science **272**, 1323 (1996).
3. A.P. Alivisatos, Science **271**, 933 (1996).
4. C.S. Lent and P.D. Tougaw, Proc. IEEE **85**, 541 (1997).
5. Devore, J.L. (1982). *Probability and Statistics for Engineering and the Statistics for Engineering and the Sciences.* Brooks/Cole Publishing Company. Monterey, California.
6. J. Garcia-Rodeja, C.J. Rey, L.J. Gallego, and J.A. Alanso, Phys. Rev. B **49**, 8495 (1994).
7. S. Erkoc and R. Shaltaf, Phys. Rev. A **60**, 3053 (1999).
8. S. Darby, T.V. Mortimer-Jones, R.L. Johnson, and C. Roberts, J. Chem. Phys. 116, 1536 (2002).
9. N.T. Wilson and R.L. Johnston, Eur. Phys. J. D **12**, 161 (2000).
10. I. Hijazi and Y. Park, J. Mater. Sci. Technol. **25,** 835 (2009).
11. M. Daw and M. Baskes, Phys. Rev. Lett. **50**, 1285 (1983).
12. B. Chen and J.I. Siepmann, J. Phys. Chem., **104**, pp. 8725 (2000).
13. H. Cox, R.L. Johnson, and J.N. Murrell, J. Solid State Chem. **145**, 517 (1999).